Cancer Research

# Ki-67 as a Molecular Target for Therapy in an *In vitro* Three-Dimensional Model for Ovarian Cancer

Ramtin Rahmanzadeh[1], Prakash Rai[1], Jonathan P. Celli[1], Imran Rizvi[1,2], Bettina Baron-Lühr[3], Johannes Gerdes[3], and Tayyaba Hasan[1]

## Abstract

Targeting molecular markers and pathways implicated in cancer cell growth is a promising avenue for developing effective therapies. Although the Ki-67 protein (pKi-67) is a key marker associated with aggressively proliferating cancer cells and poor prognosis, its full potential as a therapeutic target has never before been successfully shown. In this regard, its nuclear localization presents a major hurdle because of the need for intracellular and intranuclear delivery of targeting and therapeutic moieties. Using a liposomally encapsulated construct, we show for the first time the specific delivery of a Ki-67–directed antibody and subsequent light-triggered death in the human ovarian cancer cell line OVCAR-5. Photoimmunoconjugate-encapsulating liposomes (PICEL) were constructed from anti–pKi-67 antibodies conjugated to fluorescein 5(6)-isothiocyanate, as a photoactivatable agent, followed by encapsulation in noncationic liposomes. Nucleolar localization of the PICELs was confirmed by confocal imaging. Photodynamic activation with PICELs specifically killed pKi-67–positive cancer cells both in monolayer and in three-dimensional (3D) cultures of OVCAR-5 cells, with the antibody TuBB-9 targeting a physiologically active form of pKi-67 but not with MIB-1, directed to a different epitope. This is the first demonstration of (*a*) the exploitation of Ki-67 as a molecular target for therapy and (*b*) specific delivery of an antibody to the nucleolus in monolayer cancer cells and in an *in vitro* 3D model system. In view of the ubiquity of pKi-67 in proliferating cells in cancer and the specificity of targeting in 3D multicellular acini, these findings are promising and the approach merits further investigation. *Cancer Res; 70(22); 9234–42. ©2010 AACR.*

## Introduction

Targeted agents that block or interrupt specific pathways intricately involved in tumor growth and cancer cell proliferation hold promise for effective patient-customized treatment. The choice of the molecular target around which to design molecularly targeted therapies then becomes a key factor. In that context, the nuclear protein Ki-67 (pKi-67) is a compelling candidate. It is strongly expressed in proliferating cells (1, 2) and is an established prognostic indicator for the assessment of cell proliferation in biopsies from cancer patients (3). Despite the important role of pKi-67 as a diagnostic marker, three challenges have limited its suitability as a target for cancer therapy: (*a*) lack of targeting moieties that specifically recognize the physiologically active form of pKi-67; (*b*) lack of effective vehicles for intracellular delivery that effectively transport the targeting moiety to the appropriate subcellular site; and (*c*) the inability to link the targeting mechanism with an externally activatable intervention strategy for additional specificity that neutralizes the active state of pKi-67.

We address these challenges using a multifunctional (fluorescence and therapy) nanotechnology platform for intracellular delivery of TuBB-9, a recently developed monoclonal antibody (mAb; ref. 4) that specifically recognizes a physiologically active form of pKi-67, in combination with a photoactivatable agent in a photochemistry-based approach called photodynamic therapy (PDT). PDT involves the excitation of light-activatable chemicals to trigger site-specific photochemistry for localized damage via active molecular species, because of which very specific target damage can be achieved (5–7). In this study, we show the first antibody-targeted inactivation of a nuclear protein in large cell populations. This was made feasible through nanotechnology-derived liposomal delivery of an antibody. We subsequently present the first evidence that inactivation of the proliferation marker pKi-67 leads to cell death in proliferating cells only. Figure 1 shows the proposed schema of the targeting strategy. TuBB-9 antibody is conjugated to a PDT agent to yield a photoimmunoconjugate (PIC), which is then encapsulated into noncationic PEGylated liposomes

**Authors' Affiliations:** [1]Wellman Center for Photomedicine, Massachusetts General Hospital, Harvard Medical School, Boston, Massachusetts; [2]Thayer School of Engineering, Dartmouth College, Hanover, New Hampshire; and [3]Department of Immunology and Cell Biology, Research Center Borstel, Borstel, Germany

**Note:** Supplementary data for this article are available at Cancer Research Online (http://cancerres.aacrjournals.org/).

**Corresponding Author:** Tayyaba Hasan, Wellman Center for Photomedicine, Massachusetts General Hospital, Harvard Medical School, 40 Blossom Street, Boston, MA 02114. Phone: 617-726-6996; Fax: 617-726-8566; E-mail: thasan@mgh.harvard.edu.

**doi:** 10.1158/0008-5472.CAN-10-1190

©2010 American Association for Cancer Research.

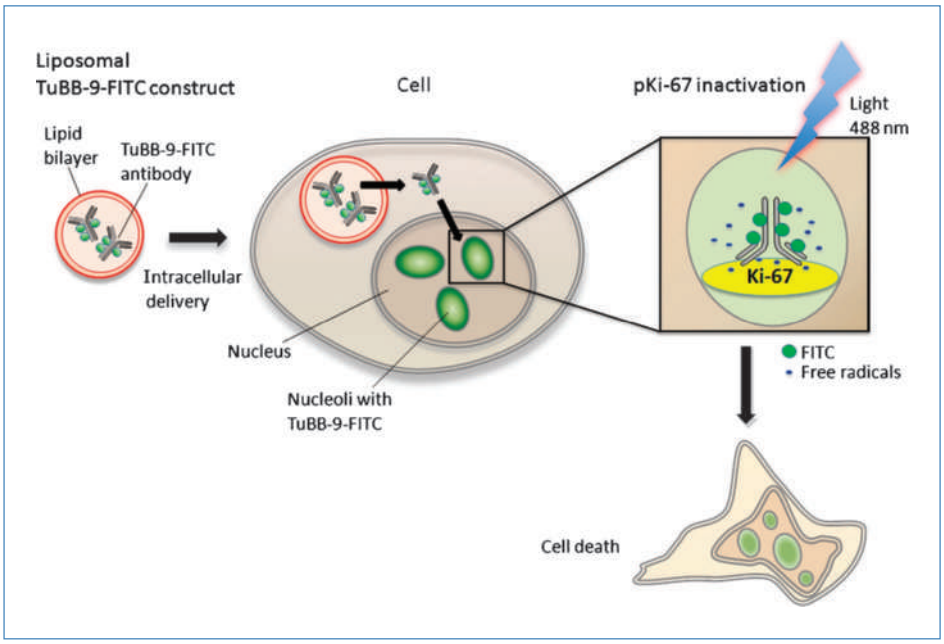


**Figure 1.** Envisioned schema showing proposed mechanism of nanotechnology-mediated subcellular antibody delivery and subsequent light inactivation of pKi-67, leading to ovarian cancer cell death. TuBB-9 antibody is conjugated to fluorescein 5(6)-isothiocyanate (FITC) to yield a PIC, which is then encapsulated into noncationic PEGylated liposomes to provide PICELs. (MIB-1–FITC conjugates are also encapsulated in liposomes and used as control but are not shown in the schema.) These PICELs are internalized by OVCAR-5 cells, and a fraction of the TuBB-9–FITC conjugates are released into the cytoplasm. Within 24 h, the conjugates relocalize into the nucleus. Proposed mechanisms for this relocalization are the cotransport of the antibody-FITC conjugates with the Ki-67 protein, after its synthesis in the cytoplasm, or binding to pKi-67 during mitosis after breakdown of the nuclear envelope. Light irradiation inactivates the Ki-67 protein and is followed by cell death of the ovarian cancer cells.

to provide PIC-encapsulating liposomes (PICEL). These are taken up by ovarian cancer cells on incubation by a combination of endocytic and liposome fusion processes. A fraction of the liposomes release the mAb into the cytoplasm of the cancer cell. Within 24 hours, the mAb relocalizes into the nucleus, consistent with earlier reports using single-cell injections (8). The putative relocalization mechanism involves the cotransport of the mAb with newly synthesized Ki-67 protein, or binding to pKi-67 during mitosis after breakdown of the nuclear envelope. Light irradiation triggers inactivation of the Ki-67 protein and cell death of the ovarian cancer cells.

Liposomes are self-assembling spherical vesicles made of lipids and have been extensively investigated for drug delivery in cancer and noncancer applications (9). Several liposomal drugs have already been approved for clinical use. The drugs that have been encapsulated in liposomes range from chemotherapeutic drugs such as doxorubicin (10) to photoactivatable agents such as benzoporphyrin derivative monoacid (11), a Food and Drug Administration (FDA)–approved PDT agent. Liposomes make it possible to intracellularly deliver large macromolecule drugs to their site of action, although the delivery of an antibody via encapsulation has never been reported. Cationic liposomes have been investigated for delivery of proteins to cells (12, 13) but initiate extreme inflammatory response and neurotoxicity (14). Here, we use noncationic PICELs for intracellular delivery of the mAbs TuBB-9 and MIB-1 recognizing pKi-67. TuBB-9 and MIB-1 are directed against different epitopes of pKi-67 and recognize pKi-67 fractions, which seem to regulate different cellular functions. These mAbs also exhibit different subnuclear staining patterns, probably caused by differential epitope masking (4).

Previous studies have shown that the fraction of pKi-67 recognized by TuBB-9 colocalizes with components of the rRNA transcription machinery and binds to the promoter region of the ribosomal genes in the nucleoli (4). Light inactivation after TuBB-9–FITC microinjection led to a profound inhibition of rRNA synthesis (15). In contrast, the rRNA synthesis machinery was independent of pKi-67 regulation when cells were microinjected with the pKi-67–recognizing mAb MIB-1. These results instigated the current investigation where we sought to exploit this reported specific inactivation of pKi-67 in single cells for cancer cell killing using PDT, which allows for an external trigger of cell death. PDT is an approved treatment modality for various malignant and nonmalignant diseases and is FDA approved as first-line treatment for age-related macular degeneration. PDT involves light-based activation of a nontoxic chemical called photosensitizer to produce cytotoxic free radicals (5–7).

In this study we use a recently developed *in vitro* three-dimensional (3D) model of disseminated ovarian micronodules as a biologically relevant research platform that is conducive to longitudinal imaging and quantitative assessment

of treatment response (16–18). This model system is adapted from the pioneering work of Bissel and colleagues (19) in breast cancer research, in which it was shown that cells overlaid on a bed of Matrigel with the proper composition of stromal factors will form multicellular 3D acini. These 3D models have led to powerful insights into the role of tissue architecture in cell signaling and tumor growth behavior that would not be possible in traditional monolayer cultures (20–22). However, the power of such systems to serve as more physiologically relevant reporters of treatment response has been underused. For example, such 3D systems recapitulate challenges for drug delivery that are similar to those encountered during i.p. administration of drugs in intra-abdominal metastatic disease. Our 3D model system generates 3D ovarian nodules that are similar in size to the micrometastatic tumor nodules studding the peritoneal surfaces *in vivo*.

Using this ovarian cancer 3D model system and monolayer cell culture, we show that epitope-specific PDT induced killing of OVCAR-5 cells with PICELs constructed from anti–pKi-67 antibodies conjugated to FITC, as a photoactivatable agent, followed by encapsulation in noncationic liposomes. This photodynamic activation with PICELs synthesized with the antibody TuBB-9 specifically killed pKi-67–positive cancer cells.

## Materials and Methods

### Antibodies and labeling

The mouse mAbs against pKi-67, MIB-1, and TuBB-9 were generated at the Research Center Borstel as described by Bullwinkel and colleagues (4) and Cattoretti and colleagues (23). For conjugation of the antibodies to FITC (fluorescein 5(6)-isothiocyanate, Sigma), FITC (2.57 mmol/L in DMSO) and antibody (6.58 μmol/L in sodium carbonate buffer) were mixed in a molar ratio of 20:1. The solution was incubated at room temperature on a shaker for 2 hours, and the labeled protein was purified with a NAP-5 Sephadex column (GE Healthcare). After elution with TBS [10 mmol/L Tris-HCl (pH 8.2), 150 mmol/L NaCl], the labeled antibodies were concentrated with Microcon tubes (Millipore) and redissolved in TBS (pH 7.4).

From the absorbance $A(\lambda)$, the protein concentration ($c_{\text{prot}}$) and the average amount of fluorochromes per antibody ($\eta$) were calculated using the formula shown below. The FITC to antibody ratios varied from 1.3 to 2.3 molecules of FITC per antibody over 10 conjugation reactions.

$$c_{\text{prot}} = \frac{A(280\text{ nm}) - 0.31 \cdot A(495\text{ nm})}{1.4}\frac{\text{mg}}{\text{mL}};$$

$$\eta = \frac{2.77 \cdot A(495\text{ nm})}{A(280\text{ nm}) - 0.31 \cdot A(495\text{ nm})}$$

### Preparation of PICELs

Liposomes encapsulating antibody conjugates were prepared by adapting the procedure described by Sengupta and colleagues (24). Briefly, the lipids (phosphatidylcholine, cholesterol, and phosphatidylethanolamine), each separately dissolved in chloroform, were mixed together in a molar ratio of 2:1:0.2 and placed in a glass vial; chloroform was evaporated from the vial under a stream of nitrogen. The residual chloroform was removed by placing this vial in a desiccator under vacuum for 1 hour. An aqueous solution of the antibody-FITC conjugate was then added at 65°C, a temperature greater than the highest value of the fluid-solid transition temperature ($T_m$) for the lipids in the mixture. The solution was incubated for 1 hour at 65°C. The resulting dispersion of multilamellar vesicles was extruded through 200-nm-diameter polycarbonate membranes by using a mini-extruder system (Avanti Polar Lipids) to form unilamellar vesicles. The resulting PICELs were then analyzed by dynamic light scattering (DLS) and transmission electron microscopy (TEM). Unencapsulated antibody-FITC conjugates were removed by gel filtration, and the concentrations were determined by fluorescence and absorbance spectroscopy.

### Cell lines and culture conditions

Human ovarian carcinoma cells NIH:OVCAR-5 (OVCAR-5) were purchased from Fox Chase Cancer Center (Philadelphia, PA), where they were characterized by microsatellite marker analysis. The cells were grown in RPMI 1640 supplemented with 10% FCS, 2% L-glutamine, and 50 units/mL penicillin/streptomycin. Human lung fibroblast cells MRC-5 were purchased from the American Type Culture Collection, where they were characterized by cytochrome oxidase I assay and inverse sequence-tagged repeat analysis. MRC-5 cells were grown in Eagle's MEM supplemented with 10% FCS, 2% L-glutamine, and 50 units/mL penicillin/streptomycin. All *in vitro* experiments were carried out with cell lines that were passaged within 6 months after initiation of the cell culture. Monolayer cells were plated for irradiation experiments on 35-mm plastic dishes (BD Biosciences). For the 3D tissue culture, OVCAR-5 cells were plated on the 14-mm glass area of 35-mm glass-bottomed dishes (MatTek). First, the glass surface was coated with 80 μL of growth factor–reduced Matrigel (BD Biosciences). The plating was fulfilled on ice because Matrigel solidifies rapidly at room temperature. After 30 minutes of incubation, 200 μL of OVCAR-5 were plated on the Matrigel bed in a concentration of 18,000 cells/mL. The culture dishes were then incubated at 37°C to allow for cell adhesion on the gel. After 1 hour, the medium volume in each dish was brought to 2 mL, containing 2% Matrigel. The 3D culture was maintained with RPMI 1640 supplemented with 2% Matrigel.

### Flow cytometric determination of the Ki-67 status

For flow cytometric analysis, cells were incubated for 5 minutes in 0.05% trypsin/EDTA. 3D cell cultures were incubated up to 30 minutes in 0.25% trypsin/EDTA. Cell suspension aliquots (500 μL, $2 \times 10^6$ cells/mL) were fixed for 10 minutes on ice by addition of 500 μL of 4% ice-cold paraformaldehyde to a final concentration of 2%. After addition of 2 mL of ice-cold PBS, cells were collected by centrifugation (400 × *g* for 5 minutes), resuspended in 500 μL of ice-cold PBS/0.25% Triton X-100, and incubated for 5 minutes on ice. Cells were then washed by adding 2 mL

of ice-cold PBS followed by centrifugation at 400 × *g*. Subsequently, the cells were then resuspended in 500 μL PBS/0.5% bovine serum albumin (BSA) containing the primary antibody MIB-1–FITC at a concentration of 2 μg/mL and incubated for 1 hour on ice in the dark. After addition of 2 mL of ice-cold PBS, cells were centrifuged at 400 × *g* and then resuspended in 500 μL PBS/0.5% BSA containing 50 μg/mL propidium iodide (to stain DNA) and 50 μg/mL RNase. Cells were incubated for an additional 30 minutes at 37°C and then analyzed on a BD FACSCalibur flow cytometer. To derive cell cycle fractions $G_1$-$G_0$, S, and $G_2$-M from DNA histograms, we took care to include only single cells in our analysis and to exclude $G_0$-$G_1$ doublets, which were discriminated using pulse height versus pulse width of the propidium iodide signal (25).

### Irradiation of monolayer and 3D culture cells

Cells were irradiated with an argon laser (Innova 100, Coherent) at 488 nm, which is in close proximity to the absorption maximum of FITC of ~494 nm. The beam was widened to a spot of 3.5-cm diameter with an irradiance of ~70 mW/cm$^2$. Irradiation energy was measured with an Ophir Vega power meter with a photodiode sensor (Ophir Optronics).

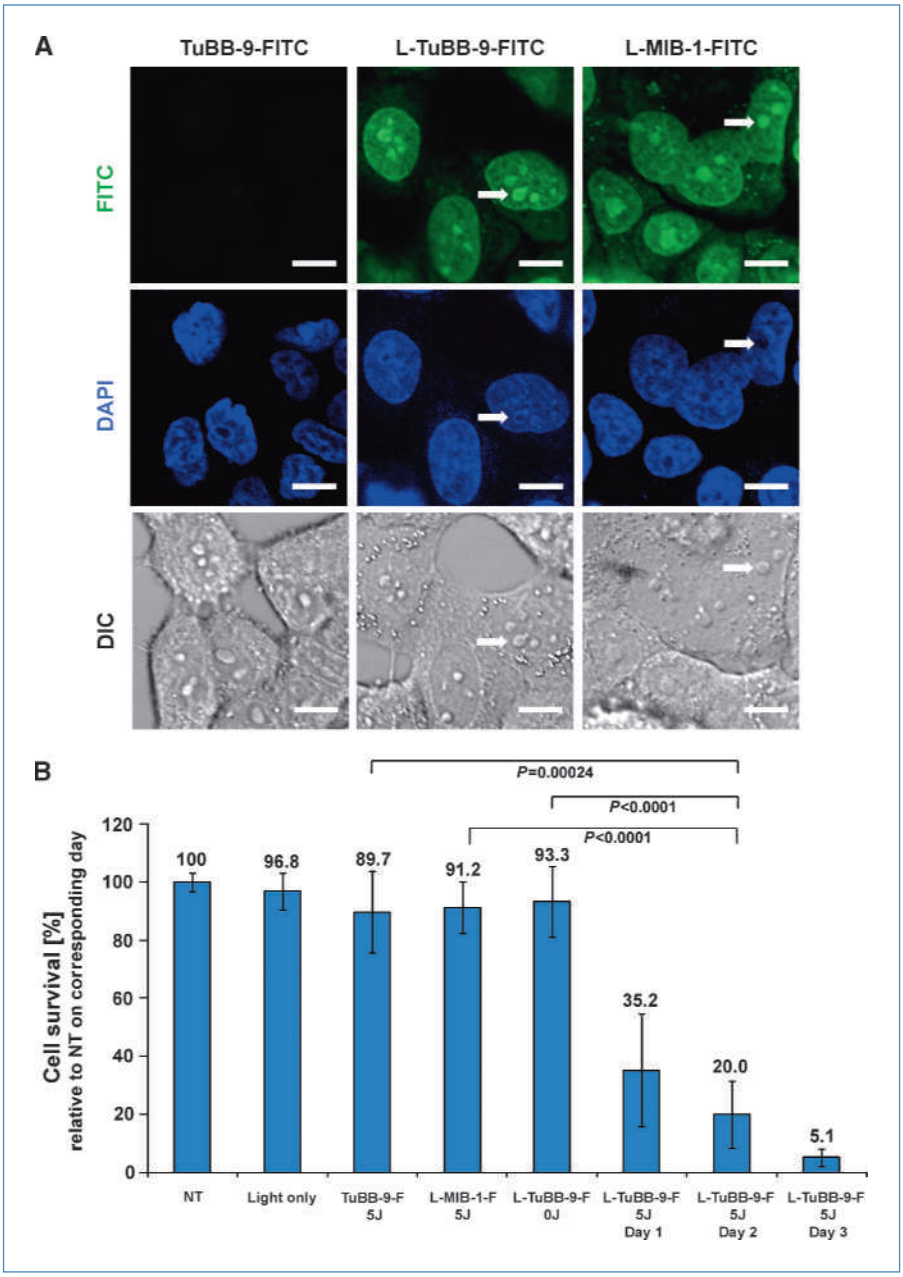


**Figure 2.** Confocal microscopy confirms subnuclear localization of anti–Ki-67–FITC antibody conjugates, and subsequent light irradiation causes ovarian cancer cell death in monolayer cultures. A, confocal laser scan images of OVCAR-5 cells 24 h after incubation with TuBB-9–FITC, L-TuBB-9–FITC, and L-MIB-1–FITC. Left, the free TuBB-9–FITC antibody conjugate without liposomal encapsulation is impermeant to the cell membrane. Both PICEL constructs L-TuBB-9–FITC (middle) and L-MIB-1–FITC (right) deliver the FITC-labeled antibody conjugates intracellularly (scale bars, 10 μm), which then localize inside the nucleoli (arrows). B, viability of OVCAR-5 cells following irradiation with a 488-nm laser (5 J/cm$^2$) is assessed by standard MTT assay. Only cells that are incubated with L-TuBB-9–FITC show a significant reduction in viability over 72 h after irradiation. Cells incubated with L-MIB-1–FITC constructs and irradiated with the same energy of light show negligible loss of viability. Negative control samples, which consist of cells without any constructs but with light irradiation, cells with L-TuBB-9–FITC constructs but no light, or cells with the free TuBB-9–FITC antibody conjugate, show no significant loss of viability.

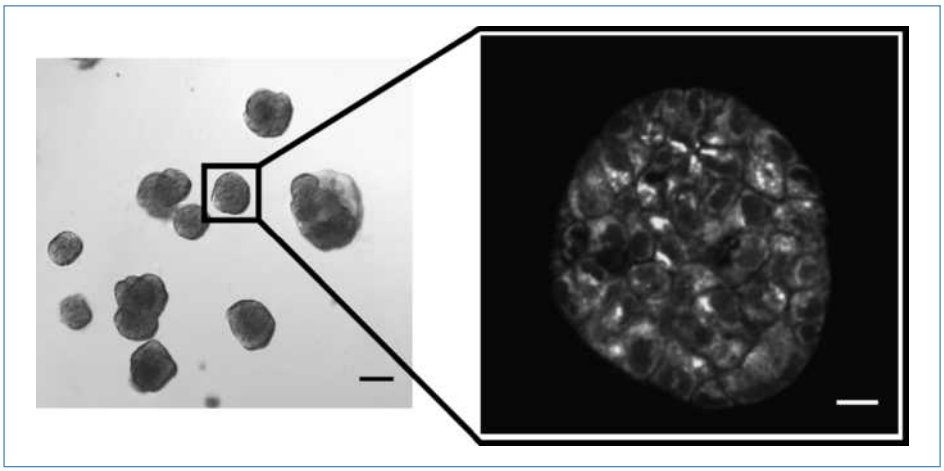

Figure 3. Multiphoton image of OVCAR-5 3D acini. The larger field of view on the left is a representative sample of 3D acini obtained by differential interference contrast microscopy. Scale bar, 100 μm. Magnified area shows a cross-section of a single acinus captured by two-photon fluorescence microscopy with excitation tuned to 750 nm to excite endogenous flavins in OVCAR-5. The autofluorescence image reveals outlines of individual cells to show the 3D cellular structure of the acinus. Scale bar, 15 μm. A z-scan through the acinus from which one section is shown is attached as Supplementary Movie.

### Multiphoton fluorescence imaging of *in vitro* 3D nodules

Images were acquired using an inverted Olympus FV1000 MPE microscope equipped with Spectra-Physics DeepSee Ti:Sapphire laser tuned to 750 nm to excite endogenous fluorescence of flavin chemical species in 3D micronodules. A 40× objective water immersion objective (Olympus) was used to acquire high-resolution images through the Matrigel bed. 3D volumes were collected by acquiring image stacks in 2-μm axial steps. Two non-descanned detectors collected the autofluorescence emission using violet (440–490 nm) and green (510–550 nm) band-pass filters. The final images and depth stack movies were processed using ImageJ. This label-free autofluorescence imaging allows nonperturbative imaging of samples without administration of exogenous contrast agents and allows cultures to be maintained for continued growth and treatment response studies. In displayed images, contrast was enhanced using hi-lo lookup table in ImageJ software. Multiphoton image data were smoothed with a 2-pixel Gaussian filter.

### Cell viability assay for monolayer and 3D culture cells

To assess cell viability in monolayer cell cultures, the MTT assay, which measures mitochondrial dehydrogenase activity, was used. Assessment of cytotoxic response in the 3D culture model posed an additional challenge, as the conversion products from traditional MTT and MTS assays were found to adhere to the Matrigel substrate, preventing reliable reporting of viability by these methods. To overcome this, we developed a quantitative fluorescence imaging–based approach using the LIVE/DEAD Cytotoxicity kit (Invitrogen). Culture dishes of 3D nodules were first washed with PBS and then incubated at 37°C for 40 minutes with 2 μmol/L calcein AM and 4 μmol/L ethidium homodimer-1 (Invitrogen) diluted in PBS before imaging. Following incubation, images of the calcein fluorescence emission (as a reporter of viability) and the ethidium bromide fluorescence emission (as a reporter of cell death) were obtained using the appropriate excitation/emission filters on an Axiovert 100 TV inverted microscope (Zeiss) at several spatial fields in each treated culture dish. Images were captured with a charge-coupled device camera (Quantifire XI, Optronix) and saved as 12-bit TIFFs for later analysis. Using a custom batch process routine developed in the MATLAB software package (MathWorks), sets of images were analyzed in high throughput to report the mean fluorescence signal from the calcein and ethidium bromide channels with the ratio of calcein fluorescence to total fluorescence (calcein plus ethidium) as a reporter of viability. The ratio was computed in this manner for all treatment groups and normalized to the no-treatment control group to calculate percentage viability for each treatment.

## Results

### PICELs deliver pKi-67 antibodies intracellularly and PDT triggers cell death of ovarian cancer cells

The PICEL constructs consisting of FITC-labeled anti–pKi-67 antibodies and a lipid bilayer were characterized by DLS to be in a size range of approximately 180 nm (see Supplementary Fig. S1). TEM images of polymer containing liposomes prepared similar to PICELs showed a spherical morphology of the liposomal constructs. There was no attempt to vary the size of the PICELs.

The subcellular localization of PICELs in OVCAR-5 cells was established by confocal laser scanning microscopy (CLSM) following a 24-hour incubation of PICELs with OVCAR-5 cells at concentrations of 20 nmol/L FITC equivalent. CLSM showed the fluorescence for both mAbs (TuBB-9

and MIB-1) to be nucleolar, coincident with the putative pKi-67 site (Fig. 2A).

To investigate if cell death was triggered by PDT, the OVCAR-5 cells incubated with PICELs for 24 hours were irradiated with an argon laser at 488 nm with 5 J/cm$^2$. MTT analysis showed a dramatic 95% decrease in cell viability with L-TuBB-9–FITC at 72 hours, whereas no significant effect on viability in cells incubated with L-MIB-1–FITC was observed. Cell viability decrease was time dependent, from 35% 24 hours after irradiation to 20% 48 hours after irradiation and to 5.15% 72 hours after irradiation (Fig. 2B). The controls show that irradiation of the non–PICEL-free TuBB-9–FITC antibody has no significant influence on cell viability. Cell viability was unaffected by irradiation of cells without any conjugate or TuBB-9 PICEL incubation without light. All experiments were done during log phase of OVCAR-5 cell growth, as shown in Supplementary Fig. S2. During this phase, the percentage of cells that stain positive for pKi-67 is the highest (26).

### 3D cultures show loss of spherical structure and increase in cell death

To evaluate efficacy of Ki-67–targeted PDT in a more biologically relevant system, we conducted treatment response studies in a 3D *in vitro* model of ovarian cancer. As shown in Fig. 3, OVCAR-5 cells grown on GFR Matrigel formed multicellular 3D acini. Supplementary Movie S1 shows a multiphoton z-scan through an acinus. Although formed from the same cell line used in monolayer experiments, molecular targets are differentially expressed when

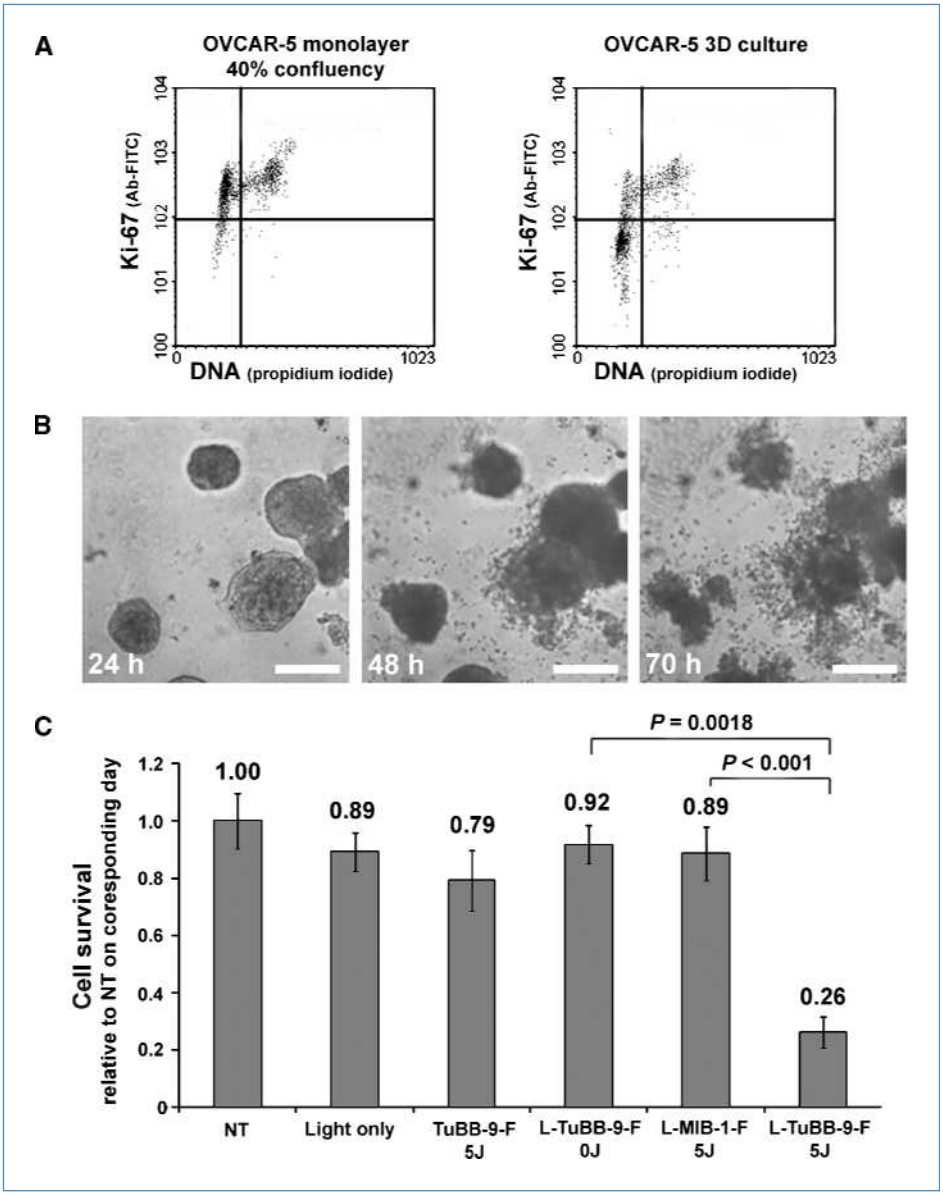


Figure 4. OVCAR-5 cells grown in 3D cultures show loss of acinar structure and a progressive increase in cell death following treatment with L-TuBB-9–FITC constructs. A, the pKi-67 expression in 3D cultures is lower than that in monolayer cultures as assessed by flow cytometry in fixed cells. B, time-lapse images of 3D cultures incubated with L-TuBB-9–FITC constructs and irradiated with 5 J/cm$^2$. The destruction of the 3D acinar structure is clearly seen 70 h after light irradiation. Scale bars, 200 μm. C, normalized live/dead ratio of 3D OVCAR-5 cells after irradiation with a 488-nm laser. The live/dead ratio decreases significantly in cells incubated with L-TuBB-9–FITC 72 h after irradiation.

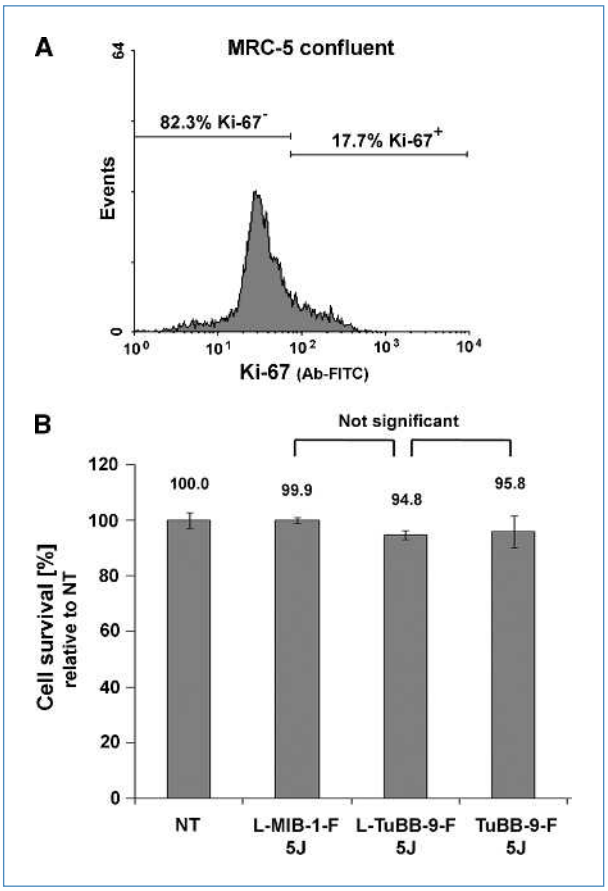


Figure 5. Treatment of a noncancer cell line, human lung fibroblast cells (MRC-5), shows the specificity of the approach for Ki-67–positive proliferating cells. A, flow cytometry for Ki-67 status in 80% confluent MRC-5 cells reveals that only a small fraction of cells is pKi-67 positive. B, viability of MRC-5 cells after irradiation with a 488-nm laser (5 J/cm$^2$) is assessed by standard MTT assay. Confluent cells with low pKi-67 expression show negligible loss of viability following incubation with both anti–pKi-67 liposomal constructs and light irradiation.

key physiologic architectural cues are restored. Flow cytometry measurements established that >90% of the cells in monolayer cultures are pKi-67 positive (Fig. 4A), whereas in 3D culture only 40% of the cells were positive for pKi-67, which is similar to the *in vivo* situation (27, 28). The expression of pKi-67 in fewer cells in 3D models compared with monolayer cells has been described before (29, 30) and is most likely the result of differential gene expression induced by differential architectural cues in the two geometries. PDT-mediated cell death triggering in 3D cultures was investigated by incubating the cultures with PICELs containing 20 nmol/L equivalent of FITC for 48 hours followed by 488-nm illumination with 5 J/cm$^2$. Time-lapse imaging over 70 hours showed a striking loss of acinar structure, which was most prominent 20 to 40 hours after irradiation (Fig. 4B; Supplementary Movies S2–S5). This disaggregation of the acini was only observed after L-TuBB-9–FITC treatment, targeting the active form of pKi-67 and not with the MIB-1 constructs. The live/dead ratio, normalized to untreated controls, decreases to 0.26 72 hours after irradiation in 3D cultures incubated with L-TuBB-9–FITC (Fig. 4C). As in monolayer, the liposomal MIB-1–FITC construct shows no significant cytotoxicity, nor did the free TuBB-9–FITC antibody or cells without any conjugate or cells treated with TuBB-9 PICELs without light irradiation.

**PDT against pKi-67 kills selectively proliferating cells**

Specificity of this approach for pKi-67–positive cells was tested in 80% confluent human lung fibroblasts (MRC-5), where only a small population of cells expresses pKi-67. Flow cytometry staining of pKi-67 in MRC-5 cells showed that cells grown to confluency expressed pKi-67 in <20% of cells (Fig. 5A), whereas nonconfluently grown cells were ~80% positive for pKi-67 (Supplementary Fig. S3A). To test the treatment efficacy on low Ki-67–expressing noncancer cells, we incubated MRC-5 cells with the PICELs and determined cell viability after light irradiation. Interestingly, the MRC-5 cells grown to confluency showed no significant effect on cell viability with either of the constructs (Fig. 5B). In contrast, nonconfluent cells showed a decrease in cell viability to 22% after 48 hours when incubated with L-TuBB-9–FITC (Supplementary Fig. S3B).

## Discussion

This study establishes the first antibody-targeted inactivation of a nucleolar protein in large populations of living cells and provides the first evidence that inactivation of the proliferation marker pKi-67 leads to cell death specifically in proliferating cells. Most protein knockdown methods interfere with the synthesis pathway of the protein (31, 32); however, here, we show a new approach for targeting the protein itself. Fabrication of the noncationic PICELs made the delivery of antibodies into the cell cytoplasm possible, leading ultimately to a relocalization of the mAbs to the actual pKi-67 site inside the nucleus and particularly in the nucleoli. This nuclear relocalization has been described earlier (8), but the exact mechanism is not known and needs to be further investigated. Our findings show the specificity of the photoinactivation, as photoactivatable FITC is delivered to the nucleoli of the cells with both antibodies, but only pKi-67 targeted with TuBB-9 constructs leads to cell death. The possible inactivation mechanism involves photo–cross-linking of the antibody with the target protein or binding partners. Singlet oxygen-dependent cross-linking after irradiation of fluorescein has been reported before and leads to oxidation of methionine side chains (15, 33, 34). The radius of inactivation of light-irradiated FITC is in the range of a few nanometers (35) and explains the high specificity of the observed effects. Although FITC has a low triplet state quantum yield and thus a very low propensity for PDT (singlet oxygen quantum yield of 3% in aqueous solution), its conjugation to antibodies apparently alters its photophysical properties such that it can be an effective PDT agent similar to malachite and indocyanine green (35, 36). In a first study such as the one presented here, the use of FITC offers several advantages, such as easy conjugation to antibodies and its

hydrophilic nature diminishes problems that may arise due to PIC aggregation. It has been widely used for specific light inactivation of proteins in living cells (35, 37). FITC has an excitation maximum of 490 nm, and although this may be well suited for cancers of the skin, it is not ideal for deep tissue-targeted photodestruction due to the fairly limited penetration of light at this wavelength. For targeting cancers of deeper tissues, use of a clinically relevant, longer-wavelength photosensitizer with a higher singlet oxygen quantum yield may seem to be more appropriate. Using such photosensitizers, the same extent of photoinactivation could be initiated with lower irradiation energies.

Previous studies have shown that only the fraction of pKi-67 recognized by TuBB-9 and not by MIB-1 is associated with the synthesis of rRNA (4) and that this synthesis was inhibited by light inactivation after TuBB-9–FITC microinjection (15). Here, we show that inactivation of pKi-67 with TuBB-9 leads to cell death in OVCAR-5 monolayer as well as in 3D cultures, and in keeping with the earlier findings, we observed a significant decrease in viable cells only when pKi-67 was targeted with TuBB-9, but not with MIB-1. pKi-67 is believed to occur in two different fractions in the cell nucleus, which are presumably associated with different binding partners and seem to regulate different cellular functions. The observed cell death may not be solely due to pKi-67 inactivation but also due to the effect of the evolving cross-links on binding partners such as the transcription factor *upstream binding factor* and its loss of function initiating subsequent cell death.

In 3D culture, our flow cytometry studies indicated that ~40% of the cells express pKi-67. Relative to nontreated control, >70% of the cells showed a loss of viability 72 hours after PDT with TuBB-9 PICELs. PDT with TuBB-9 PICELs initiates cell death in proliferating cells, and this could prevent further growth relative to the nontreated control, where the proliferating cells continue to divide and grow over 72 hours. These data are consistent with the more pronounced loss in viability seen over 3 days with the TuBB-9 PICELs PDT. Another factor that most likely increases cell death observed is the bystander effect, where cells, which are in close proximity to affected cells, can be indirectly affected as well. Bystander responses, induced by defusing mediators, have been well described after photodynamic treatment (38). In a 3D model, these effects would be far more pronounced than in monolayer cultures because the bystander effects can propagate in all three dimensions. The 3D spheres in our ovarian cancer 3D model are similar to tumor nodules in the human disease, which often occur as regrowth after tumor debulking. The observed profound structural degradation of tumor nodules in 3D culture after pKi-67 PDT is encouraging and provides interesting possibilities for combination treatments with chemotherapeutic agents, where drug penetration into the acini is a barrier.

In conclusion, the results of the study suggest for the first time that pKi-67 is potentially an attractive therapeutic target in cancer, in addition to being a prognostic marker. Due to the ubiquitous expression in all proliferating cells and the prognostic value of the Ki-67 index in many cancers, inactivation of pKi-67 could be a promising strategy for the treatment not only of ovarian cancer but also of numerous malignancies. Noncationic PICELs are particularly useful for the subcellular delivery of mAbs and also provide multifunctional constructs for imaging and therapy, which may be exploited further for encapsulating multiple compartmentalized agents. A broader significance of this study is that it provides a platform for targeting of other nuclear proteins that may regulate cell proliferation, such as histones and transcription factors. The application of light for specific inactivation of proteins in living cells has been reported before for pKi-67 and other proteins (15, 36), although associated cell killing was never shown. PDT, a photochemistry-based approach, is an approved treatment for many pathologies and also in early or advanced clinical trials for others. This externally triggered modality provides an additional level of selectivity of cell killing due to the confinement of damage only to tissue exposed to light. This overall approach combining PDT with pKi-67 targeting holds promise as an effective cancer therapy and merits further development, requiring testing in more sophisticated *in vitro* models and appropriate *in vivo* models with longer-wavelength photosensitizers.

## Disclosure of Potential Conflicts of Interest

J. Gerdes has declared financial interests with regard to sales of mAbs. All other authors do not have any financial interests.

## Acknowledgments

We thank J. Zhao, B. Farinelli, M. Purschke, and J. Bullwinkel for their assistance.

## Grant Support

NIH grant 5R01 CA119388-03 and American Recovery and Reinvestment Act grant RC1CA146337. R. Rahmanzadeh acknowledges support from Deutsche Forschungsgemeinschaft grant Ra1771/1-1.

The costs of publication of this article were defrayed in part by the payment of page charges. This article must therefore be hereby marked *advertisement* in accordance with 18 U.S.C. Section 1734 solely to indicate this fact.

Received 04/06/2010; revised 06/03/2010; accepted 07/07/2010; published OnlineFirst 11/02/2010.

## References

1. Gerdes J, Schwab U, Lemke H, Stein H. Production of a mouse monoclonal antibody reactive with a human nuclear antigen associated with cell proliferation. Int J Cancer 1983;31:13–20.
2. Gerdes J, Lemke H, Baisch H, Wacker HH, Schwab U, Stein H. Cell cycle analysis of a cell proliferation-associated human nuclear antigen defined by the monoclonal antibody Ki-67. J Immunol 1984;133:1710–5.
3. Scholzen T, Gerdes J. The Ki-67 protein: from the known and the unknown. J Cell Physiol 2000;182:311–22.
4. Bullwinkel J, Baron-Lühr B, Lüdemann A, Wohlenberg C, Gerdes J,

Scholzen T. Ki-67 protein is associated with ribosomal RNA transcription in quiescent and proliferating cells. J Cell Physiol 2006; 206:624–35.
5. Hasan T, Ortel B, Moor ACE, Pogue B. Photodynamic therapy of cancer. In: Kufe DW, Pollock RE, Weichselbaum RR, et al., editors. Cancer medicine. 6th ed. Hamilton (Ontario): BC Dekker, Inc.; 2003, p. 605–22.
6. Hasan T, Ortel B, Solban N, Pogue B. Photodynamic therapy of cancer. In: Kufe DW, Bast RC, Jr., Hait WN, et al., editors. Cancer medicine. 7th ed. Hamilton (Ontario): BC Decker, Inc.; 2006, p. 537–48.
7. Price M, Reiners JJ, Santiago AM, Kessel D. Monitoring singlet oxygen and hydroxyl radical formation with fluorescent probes during photodynamic therapy. Photochem Photobiol 2009;85: 1177–81.
8. Heyden T. Zellbiologische Untersuchungen zu intrazellulärem Transport, Funktion und Regulation des proliferations-assoziierten Antigens Ki-67 [dissertation]. Berlin (Germany): Freie Universität Berlin; 1997.
9. Torchilin VP. Recent advances with liposomes as pharmaceutical carriers. Nat Rev Drug Discov 2005;4:145–60.
10. Tejada-Berges T, Granai CO, Gordinier M, Gajewski W. Caelyx/Doxil for the treatment of metastatic ovarian and breast cancer. Expert Rev Anticancer Ther 2002;2:143–50.
11. Schmidt-Erfurth U, Hasan T. Mechanisms of action of photodynamic therapy with verteporfin for the treatment of age-related macular degeneration. Surv Ophthalmol 2000;45:195–214.
12. Zelphati O, Szoka FC. Mechanism of oligonucleotide release from cationic liposomes. Proc Natl Acad Sci U S A 1996;93:11493–8.
13. Zelphati O, Wang Y, Kitada S, Reed JC, Felgner PL, Corbeil J. Intracellular delivery of proteins with a new lipid-mediated delivery system. J Biol Chem 2001;276:35103–10.
14. Filion MC, Phillips NC. Major limitations in the use of cationic liposomes for DNA delivery. Int J Pharm 1998;162:159–70.
15. Rahmanzadeh R, Hüttmann G, Gerdes J, Scholzen T. Chromophore-assisted light inactivation of pKi-67 leads to inhibition of ribosomal RNA synthesis. Cell Prolif 2007;40:422–30.
16. Zhong W, Celli JP, Rizvi I, et al. *In vivo* high-resolution fluorescence microendoscopy for ovarian cancer detection and treatment monitoring. Br J Cancer 2009;101:2015–22.
17. Evans CL, Rizvi I, Hasan T, de Boer JF. *In vitro* ovarian tumor growth and treatment response dynamics visualized with time-lapse OCT imaging. Opt Express 2009;17:8892–906.
18. Celli JP, Rizvi I, Evans CL, Abu-Yousif AO, Hasan T. Quantitative imaging reveals heterogeneous growth dynamics and treatment-dependent residual tumor distributions in a 3D ovarian cancer model. J Biomed Opt 2010;15:DOI: 10.1117/1.3483903.
19. Bissell MJ, Weaver VM, Lelievre SA, Wang F, Petersen OW, Schmeichel KL. Tissue structure, nuclear organization, and gene expression in normal and malignant breast. Cancer Res 1999;59: 1757–63.
20. Bissell MJ, Radisky D. Putting tumours in context. Nat Rev Cancer 2001;1:46–54.
21. Debnath J, Brugge JS. Modelling glandular epithelial cancers in three-dimensional cultures. Nat Rev Cancer 2005;5:675–88.
22. Griffith LG, Swartz MA. Capturing complex 3D tissue physiology *in vitro*. Nat Rev Mol Cell Biol 2006;7:211–24.
23. Cattoretti G, Becker MH, Key G, et al. Monoclonal antibodies against recombinant parts of the Ki-67 antigen (MIB-1 and MIB-3) detect proliferating cells in microwave-processed formalin-fixed paraffin sections. J Pathol 1992;168:357–63.
24. Sengupta S, Eavarone D, Capila I, et al. Temporal targeting of tumour cells and neovasculature with a nanoscale delivery system. Nature 2005;436:568–72.
25. Weisheit G, Gliem M, Endl E, Pfeffer PL, Busslinger M, Schilling K. Postnatal development of the murine cerebellar cortex: formation and early dispersal of basket, stellate and Golgi neurons. Eur J Neurosci 2006;24:466–78.
26. Endl E, Kausch I, Baack M, Knippers R, Gerdes J, Scholzen T. The expression of Ki-67, MCM3, and p27 defines distinct subsets of proliferating, resting, and differentiated cells. J Pathol 2001;195: 457–62.
27. Isola J, Kallioniemi OP, Korte JM, et al. Steroid receptors and Ki-67 reactivity in ovarian cancer and in normal ovary: correlation with DNA flow cytometry, biochemical receptor assay, and patient survival. J Pathol 1990;162:295–301.
28. Garzetti GG, Ciavattini A, Goteri G, et al. Ki67 antigen immunostaining (MIB 1 monoclonal antibody) in serous ovarian tumors: index of proliferative activity with prognostic significance. Gynecol Oncol 1995;56:169–74.
29. Debnath J, Mills KR, Collins NL, Reginato MJ, Muthuswamy SK, Brugge JS. The role of apoptosis in creating and maintaining luminal space within normal and oncogene-expressing mammary acini. Cell 2002;111:29–40.
30. Coppock HA, Gilham DE, Howell A, Clarke RB. Cyclin-dependent kinase inhibitors and basement membrane interact to regulate breast epithelial cell differentiation and acinar morphogenesis. Cell Prolif 2007;40:721–40.
31. Kausch I, Lingnau A, Endl E, et al. Antisense treatment against Ki-67 mRNA inhibits proliferation and tumor growth *in vitro* and *in vivo*. Int J Cancer 2003;105:710–6.
32. Kausch I, Jiang H, Brocks C, et al. Ki-67-directed antisense therapy in an orthotopic renal cell carcinoma model. Eur Urol 2004;46: 118–24.
33. Lepock JR, Thompson JE, Kruuv J. Photoinduced crosslinking of membrane proteins by fluorescein isothiocyanate. Biochem Biophys Res Commun 1978;85:344–50.
34. Yan P, Xiong Y, Chen B, Negash S, Squier TC, Mayer MU. Fluorophore-assisted light inactivation of calmodulin involves singlet-oxygen mediated cross-linking and methionine oxidation. Biochemistry 2006;45:4736–48.
35. Surrey T, Elowitz MB, Wolf PE, et al. Chromophore-assisted light inactivation and self-organization of microtubules and motors. Proc Natl Acad Sci U S A 1998;95:4293–8.
36. Liao JC, Roider J, Jay DG. Chromophore-assisted laser inactivation of proteins is mediated by the photogeneration of free radicals. Proc Natl Acad Sci U S A 1994;91:2659–63.
37. Beck S, Sakurai T, Eustace BK, et al. Fluorophore-assisted light inactivation: a high-throughput tool for direct target validation of proteins. Proteomics 2002;2:247–55.
38. Chakraborty A, Held KD, Prise KM, Liber HL, Redmond RW. Bystander effects induced by diffusing mediators after photodynamic stress. Radiat Res 2009;172:74–81.